ISSN 1070-3632, Russian Journal of General Chemistry, 2016, Vol. 86, No. 3, pp. 708–717. © Pleiades Publishing, Ltd., 2016.

Synthesis, Spectroscopic, and Antimicrobial Study of Ca(II), Fe(III), Pd(II), and Au(III) Complexes of Amoxicillin Antibiotic Drug[1]

F. A. I. Al-Khodir[a,b] and M. S. Refat[c,d]

[a] *Department of Chemistry, College of Science, Princess Nora Bint Abdul Rahman University, Riyadh, Saudi Arabia*

[b] *Deanship of Scientific Research, Princess Nora Bint Adul Rahman University, Riyadh, Saudi Arabia*

[c] *Department of Chemistry, Faculty of Science, Port Said, Port Said University, Egypt*

[d] *Department of Chemistry, Faculty of Sciences, Taif University, Al-Haweiah, P.O. Box 888, Taif, 21974 Saudi Arabia*
e-mail: msrefat@yahoo.com

Received September 18, 2015

Abstract—Synthesis, spectroscopic characterization, theoretical and antimicrobial studies of Ca(II), Fe(III), Pd(II), and Au(III) complexes of amoxicillin (amox) antibiotic drug are presented in the current paper. Structure of 1 : 1 (metal : amox) complexes were elucidated on the basis of elemental analyses, and IR, Raman, ^{1}H NMR, and electronic spectral data. According to molar conductance measurements the complexes had electrolyte nature. Amoxicillin reacted with metal ions as a tridentate ligand coordinated with metal ions via $–NH_2$, –NH, and β-lactam carbonyl groups. The complexes were formulated as $[Ca(amox\text{-}Na)(H_2O)]\cdot Cl_2\cdot 4H_2O$ (**1**), $[Fe(amox\text{-}Na)(H_2O)_3]\cdot Cl_3\cdot 3H_2O$ (**2**), $[Pd(amox\text{-}Na)(H_2O)]\cdot Cl_2$ (**3**), and $[Au(amox\text{-}Na)(H_2O)]\cdot Cl_3$ (**4**). Kinetic thermodynamic parameters (E^*, ΔS^*, ΔH^*, and ΔG^*) were calculated based on the Coats–Redfern and Horowitz–Metzger methods using thermo gravimetric curves of TG and DTG. Nanosize particles of amoxicillin complexes have been studied by XRD, SEM, and TEM methods. Theoretical studies of the synthesized complexes have been performed.

Keywords: antibiotics, amoxicillin, chelation, spectroscopy, anticancer activity, nanosize

DOI: 10.1134/S1070363216030324

INTRODUCTION

Metal-drug complexes have received considerable attention recently [1–6] because metal-drug chelation causes significant changes in the biological properties of ligands [3, 5]. Formation of metalloantibiotic skeletons demonstrated to be an efficient enhancement of biological and medical activity [7–10]. According to literature survey, the great attention has been drawn to studies of the antitumor activity of inorganic complexes [11, 12]. Transfer of metal ions from a ligand to the viruses associated with cancer is a possible mechanism for releasing the anticancer drug in the locality of the tumor [12].

Amoxicillin (Fig. 1) is an analog of ampicillin, derived from the basic penicillin nucleus [13–15]. β-Lactamic antibiotics possess a number of potential donor sites that can interact efficiently with metal ions and organometallic moieties [16–19] giving complexes characterized by high biological and pharmaceutical activity [20–22].

Amoxicillin mixed ligand copper complexes were synthesized [23] and their anti-bacteria [24] and protein synthesis inhibiting activity [25–28] were reported. Amoxicillin antibiotic demonstrated some

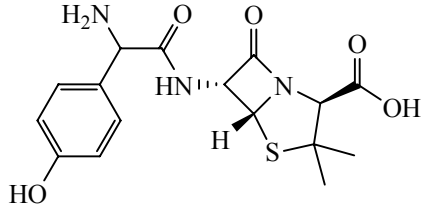

Fig. 1. Amoxicillin (amox) antibiotic drug.

[1] The text was submitted by the authors in English.

effect against urinary tract infections and is used in treatment of respiratory infections and meningitis [29]. Structure and other characteristics of amoxicillin complexes with various metals were studied extensively [30–39].

In continuation of our research of metal-drug interactions [40–45], the current study targeted synthesis, theoretical calculations, spectroscopic characterization, thermal stability assessment, and biological evaluation of amoxicillin antibiotic drug complexes with Ca(II), Fe(III), Pd(II), and Au(III) ions.

EXPERIMENTAL

Amoxicillin trihydrate antibiotic drug was received from Aldrich Chemical Company. All chemicals used were of analytical reagent grade obtained from BDH and used without additional purification.

Synthesis. Ca(II), Fe(III), Pd(II), and Au(II) amoxicillin complexes were prepared in a similar way according to the following procedure: 1.0 mmol of amoxicillin trihydrate was dissolved in 25 mL of methanol and mixed with 25 mL of methanolic solution of 1 mmol of one of salts: $CaCl_2$, $FeCl_3 \cdot 6H_2O$, $PdCl_2$, or $NaAuCl_4 \cdot 2H_2O$. A mixture of 1 : 1 molar ratio (metal ion : amox) at pH 7–8, adjusted by 1 M of NaOH in methanol, was refluxed under continuous stirring for ca. 2 h. The mixture was left overnight. The precipitate formed was filtered off and washed with methanol and dried over anhydrous calcium chloride. The yield of products collected was in the range 68–76%.

Instruments. CHN analysis was carried out by Vario EL Fab analyzer. Content of water and metals was determined by gravimetric analysis. IR spectra were recorded on a Bruker IR spectrophotometer in the range of 400–4000 cm^{-1}. Raman spectra were recorded on a Bruker FT-Raman with the laser 50 mW. Molar conductance of 10^{-3} M solutions of the complexes in DMSO were measured on a HACH conductivity meter. All measurements were taken at room temperature for freshly prepared solutions. Electronic spectra of the complexes were measured in DMSO solution, concentration 1×10^{-3} M, in the range of 200–800 nm on a Unicam UV–Vis spectrophotometer. Effective magnetic moments (μ_{eff}) of complexes were measured at room temperature using Gouy's method by a magnetic susceptibility balance, Johnson Metthey and Sherwood model. ^{1}H NMR spectra were measured in DMSO solutions on a Bruker 600 MHz spectrometer using TMS as the internal standard. Thermogravimetric analysis (TGA) was conducted on a Shimadzu TGA-50H thermal analyzer. All experiments were performed using a single loose top loading platinum sample pan under the atmosphere of nitrogen at a flow rate of 30 mL/min and a 10°C/min heating rate within the temperature range of 25–800°C. SEM images were obtained using a Jeol Jem-1200 EX II Electron microscope at an acceleration voltage of 25 kV. X-ray diffraction (XRD) patterns of the samples were recorded on Philips X Pert X-ray diffractometer using Cu$K_{\alpha 1}$ radiation with a graphite monochromator at 0.02°/min scanning rate. TEM images were recorded on a JEOL 100s microscope.

Antimicrobial assessments. Antimicrobial activity of the samples was determined using the modified Kirby–Bauer disc diffusion method [46–51]. Plates were inoculated with filamentous fungi *Aspergillus Flavus* at 25°C for 48 h. Gram (+) bacteria *Staphylococcus Aureus, Bacillus subtilis* and Gram (–) bacteria *Escherichia Coli*, *Pseudomonas aeruginosa* were incubated at 35–37°C for 24–48 h. Yeast *Candida Albicans* were incubated at 30°C for 24–48 h. Standard discs of tetracycline (antibacterial agent), amphotericin B (antifungal agent) served as positive controls for antimicrobial activity. Filter disc impregnated with 10 μL of solvent (distilled water and DMSO) were used as the negative control. Meuller-Hinton agar composition and pH were rigorously tested. Diameter of disc diffusion zones were measured with slipping calipers of the Clinical Laboratory Standers [48]. Agar based methods such as Etest disk diffusion could be good alternatives being the simpler and faster than broth methods [52, 53].

Anti-cancer activity. Human colon carcinoma (HCT-116) cells and human hepatocellular carcinoma (HepG-2) cells were obtained from the American type culture collection ATCC, Rockvill, MD. The cells were grown on RPMI-1640 medium supplemented with 10% inactivated fetal calf serum and 50 μg/mL gentamycin. The cells were stored at 37°C in the humidified atmosphere with 5% CO_2 and subcultured 2–3 times a weak. The cells were grown as monolayers in growth RPMI-1640 medium supplemented with 10% inactivated fetal calf serum and 50 μg/mL gentamycin. The monolayers of 10000 cells adhered at the bottom of the wells in a 96-well micro titer plate were incubated for 24 h at 37°C in a humidified incubator with 5% CO_2. The monolayers were washed with sterile phosphate buffered saline (0.01 M, pH =

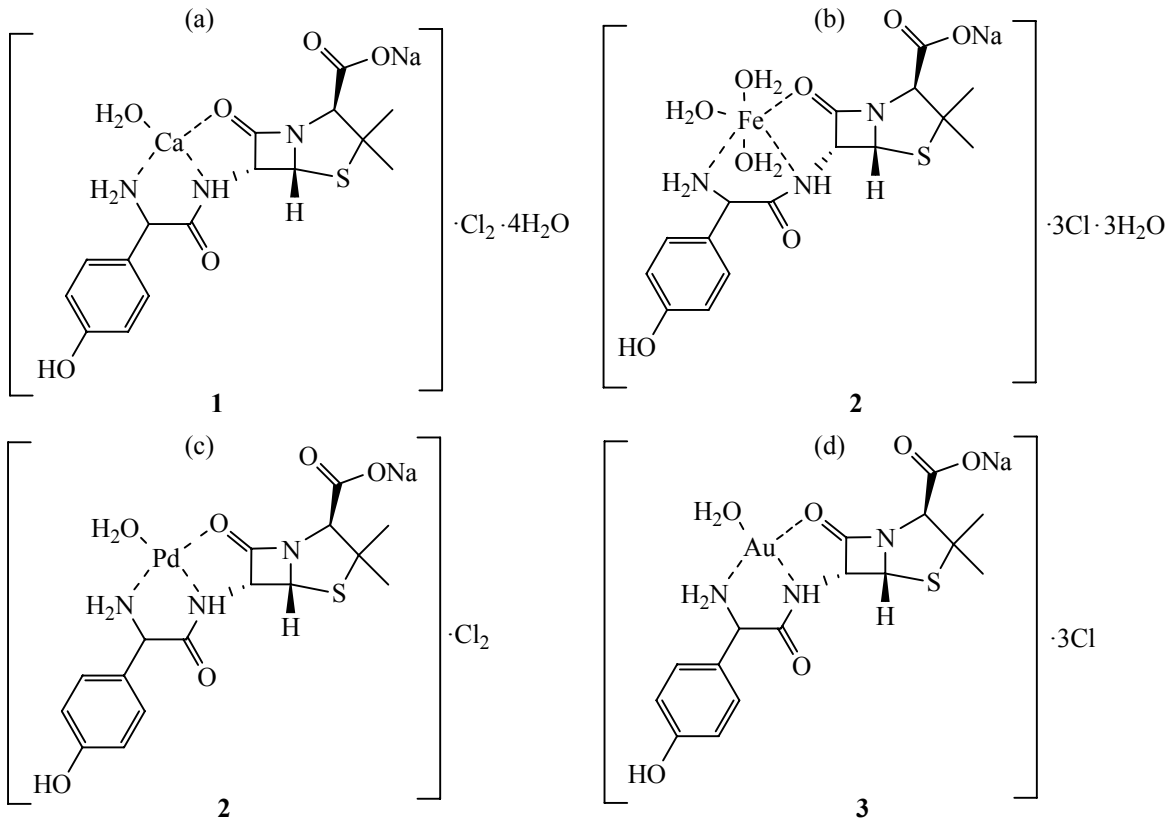

Fig. 2. Suggested formulas of [Ca(amox-Na)(H_2O)]·Cl_2·4H_2O (**1**), [Fe(amox-Na)(H_2O)$_3$]·Cl_3·3H_2O (**2**), [Pd(amox-Na)(H_2O)]·Cl_2 (**3**), and [Au(amox-Na)(H_2O)]·Cl_3 (**4**) complexes.

7.2) and simultaneously the cells were treated with 100 μL fractions taken from different dilutions of the test samples in fresh maintenance medium and incubated at 37°C. Control of untreated cells was made in the absence of a test sample. Six wells were used for each concentration of the test sample. Every 24 h observation under the inverted microscope was made. The number of the surviving cells was determined by staining the cells with crystal violet [54, 55] followed by cell lysing using 33% glacial acetic acid and the absorbance recorded at 490 nm using ELISA reader (Sun Rise, TECAN, Inc, USA) upon efficient mixing. Absorbance values determined for untreated cells were considered as 100% proliferation. The number of viable cells was determined using ELISA reader as previously mentioned and the percentage of viability was calculated as [1 – (ODt/ODc)] × 100%, where ODt is the mean optical density of wells treated with the test sample and ODc is the mean optical density of untreated cells. The 50% inhibitory concentration (IC_{50}) was estimated from graphic plots.

RESULTS AND DISCUSSION

Analytical and physical data. Analytical and spectral data (Table 1) accumulated for the metals complexes indicated 1 : 1 (metal : amox) stoichiometry and the corresponding formulas to be as follows: [Ca(amox-Na)(H_2O)]·Cl_2·4H_2O, [Fe(amox-Na)(H_2O)$_3$]·Cl_3·3H_2O, [Pd(amox-Na)(H_2O)]·Cl_2 and [Au(amox-Na)(H_2O)]·Cl_3 (Fig. 2). Electrolytic characteristics [56] of amox complexes were influenced by the presence of chloride ions outside the coordination sphere. Magnetic moments of amox complexes were measured at room temperature indicated their diamagnetic character, except for [Fe(amox-Na)(H_2O)$_3$]·Cl_3·3H_2O complex which demonstrated the paramagnetic character.

IR and Raman spectra. In IR spectra the broad band at ca 3400 cm^{-1} was assigned to fixed water molecules. Free amox was characterized by two bands at 3461 and 3187 cm^{-1} assigned to ν(O–H) and ν(N–H) [57]. The bands were absent or shifted to lower wave

Table 1. Elemental analysis and physical data of free amox and its metal complexes

Complex	Color	mp, °C	Λ_m, mS	Elemental analysis, %									
				found					calculated				
				C	H	N	Cl	M	C	H	N	Cl	M
Amox	White	>200	12	52.59	5.24	11.50	–	–	–	–	–	–	–
1	Yellowish white	>250	102	32.27	4.79	7.47	11.98	6.55	32.66	4.80	7.14	12.05	6.81
2	Dark brown	>250	229	29.93	4.92	6.43	16.08	8.31	29.22	4.60	6.39	16.17	8.49
3	Brown	>250	121	32.49	3.53	6.83	12.06	18.10	32.98	3.46	7.21	12.17	18.26
4	Dark brown	>250	242	26.76	2.45	5.66	14.93	27.64	27.11	2.84	5.93	15.01	27.79

numbers in the spectra of amox complexes due to sharing the donation sites in the process of coordination with metal ions. The carbonyl group band (1776 cm^{-1}) of β-lactam ring of free amox was absent or shifted to lower wavenumbers in IR spectra of the amox complexes due to the group involvement in the coordination toward metal ion [58]. The amido group band at 1687 cm^{-1} of the free amox was shifted to lower wavenumbers at 1667, 1606, 1611, and 1605 cm^{-1} for the Ca(II), Fe(III), Pd(II), and Au(III) complexes, respectively, indicating that the amido group was involved in coordination. The carboxylic group bands indicated ionization of the group in the complexes synthesized [59]. IR data supported the fact that amox acted as the 1 : 1 tridentate ligand molecule with Ca(II), Fe(III), Pd(II), and Au(III) ions via amino, amido and β-lactam groups.

Electronic spectra and magnetic measurements. UV-Vis absorption spectra of Fe(III) complex demonstrated π→π* transitions at 280 and 300 nm due to aromaticity of the double bonds [60, 61]. The n→π* transitions were recorded at 320, 355, 370, and 400 nm assigned to β-lactam, carboxylate, amino, amido, and dimethyl thiazolidine groups [62]. The Fe(III)- amox complex had high spin indicated by two absorption bands at 400 and 320 nm due to ${}^6A_{1g}\rightarrow{}^4T_{2g}$ and ${}^6A_{1g}\rightarrow{}^4T_{1g}$ transitions, respectively [63, 64]. The third band at 280 nm was assigned to M→L and L→M charge transfer. Magnetic moment of the complex, 5.21 B.M., was supporting its octahedral geometry [65, 66]. Magnetic moments of Ca(II), Pd(II) and Au(III) complexes at room temperature indicated their diamagnetic character. The Au(III) complex was also of diamagnetic nature as could be expected for low spin d^8 complexes associated with square planar geometry [67].

^{1}H NMR spectra. The signals of Ca(II) and Pd(II) complexes at 3.367 and 3.342 ppm, respectively, were assigned to water molecules inside the coordination sphere (Table 3). Disapearance of $–NH_2$ protons signals (2.499 ppm in free amox) in Ca(II) and Pd(II) complexes spectra was due to the involvement of nitrogen of the amino group in complexation. The signals of H_b, H_c, H_a, and H_d in spectra of the complexes were shifted to high field [68] due to possible alteration in electronic configuration of amox upon complexation (Scheme 1).

Table 2. Free amox and its complexes IR/Raman spectral bands and their assignments

Amox	Ca(II)	Fe(III)	Pd(II)	Au(III)	Assignments
3461	3413	3410	3415	3400	ν(OH); COOH + H_2O
3187	–	–	–	–	ν(NH)
1776	1731	–	–	–	ν(C=O); β-lactam
1687	1667	1606	1611	1605	ν(C=O); amido group
–	1516	1511	1513	1510	ν_{as}(COO)
–	1252	1275	1273	1275	ν_s(COO)
–	264	236	240	235	$\Delta\nu = [\nu_{as}(COO) – \nu_s(COO)]$
–	568, 535	547	569	569, 532	ν(M–O)
–	430	436	445	451	ν(M–N)
–	552	541	560	542	ν(M–O); Raman
–	442	450	440	437	ν(M–N); Raman

Table 3. ^{1}H NMR spectral data of free amox and its Ca(II) and Pd(II) complexes

Assignments	δ, ppm		
	amox	Ca(II)	Pd(II)
Aromatic protons	6.741, 7.231	6.721, 7.271	6.821, 7.311
–NH–CO	8.861	8.561	8.405
NH_2	2.499	–	–
CH_3	1.514	1.574	0.895
H_b	5.454	5.140	4.821
H_c	5.370	4.800	3.878
H_a	5.356	4.700	3.616
H_d	4.045	3.640	3.370
H_2O	–	3.367	3.342

Thermal analysis. In accordance with thermo gravimetric data degradation steps of the complexes are summarized in Table 4.

The kinetic thermodynamic parameters were theoretically estimated by the integral Coats & Redfern method [69] (Table 5). The relationships used: $\Delta H = E - RT$, $\Delta S = R[\ln (Ah/kT)]$, and $\Delta G = \Delta H - T\Delta S$, where k is the Boltzmann's constant and h is the Planck's constant.

Correlation coefficients of the Arrhenius plots of thermal decomposition steps were found to be in the range of 0.9960 to 0.9990, demonstrating a good fit with the linear function. Thermal decomposition processes of all amox complexes were non-spontaneous indicating thermal stability of the complexes [70, 71].

Scheme 1. Proton arrangement and chemical shifts (ppm) of amox.

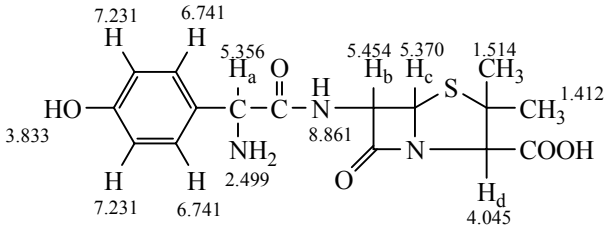

X-ray powder diffraction, SEM and TEM studies. X-ray diffraction patterns of Au(III) complex had the crystalline fashion. The grain sizes calculated with the Deby–Scherrer formula [72] were found to be 155 and 4.30 nm for free amox and Au(III) complex, respectively. The lower grain size of Au(III) complex could be interpreted in terms of increasing chelation around metal ions (ratio 1 : 1) [73]. XRD data are presented in Table 6. The crystallite sizes (D) were calculated using the Scherrer formula from the full-width half-maximum (FWHM) (β). The strain ($\varepsilon = 0.318 \times 10^{-4}$) was calculated from the slope of $\beta \cos\theta$ versus $\sin\theta$ plot using the equation:

$$\beta = \frac{\lambda}{D\cos\theta} - s\tan\theta.$$

The dislocation density ($\delta = 0.054 \times 10^{12}$ lin/m^2) (Table 6) was evaluated using the equation [74]: $\delta = 1/D^2$.

According to SEM image (Fig. 3) of the Au(III) complex, its structure was uniform in shape.

Table 4. Thermogravimetric data of the amox complexes

Complex	Steps	Temperature range, °C	Assignments	Weight loss, %	
				found	calculated
Ca(II)	1	50–207	$4H_2O$	12.71	12.23
	2	207–800	$H_2O + Cl_2$ + amox-Na	77.48	78.24
	Residue		CaO	9.81	9.53
Fe(III)	1	50–158	$3H_2O$	8.22	8.21
	2	158–800	$HCl + Cl_2 + 3H_2O$ + amox-Na	66.79	67.51
	Residue		$FeO_{1/2}$	24.99	24.28
Pd(II)	1	25–800	$Cl_2 + H_2O$ + amox-Na	79.75	78.99
	Residue		PdO	20.25	21.01
Au(III)	1	25–800	$HCl + Cl_2 + H_2O$ + amox-Na	72.02	72.21
	Residue		Au metal	27.98	27.79

Table 5. Kinetic parameters for the amox complexes based on the Coats–Redfern method

Complexes	DTG_{max}	Thermodynamic parameters	
		parameters	values
Ca(II)	260°C	E, kJ/mol	105
		A, s^{-1}	9.30×10^8
		ΔS, J mol^{-1} K^{-1}	–76
		ΔH, kJ/mol	100
		ΔG, kJ/mol	120
		r	0.9960
Fe(III)	300°C	E, kJ/mol	205
		A, s^{-1}	5.00×10^{18}
		ΔS, J mol^{-1} K^{-1}	–104
		ΔH, kJ/mol	201
		ΔG, kJ/mol	175
		r	0.9970
Pd(II)	270°C	E, kJ/mol	220
		A, s^{-1}	4.50×10^{18}
		ΔS, J mol^{-1} K^{-1}	–104
		ΔH, kJ/mol	214
		ΔG, kJ/mol	185
		r	0.9990
Au(III)	320°C	E, kJ/mol	240
		A, s^{-1}	7.00×10^{19}
		ΔS, J mol^{-1} K^{-1}	–128
		ΔH, kJ/mol	230
		ΔG, kJ/mol	192
		r	0.9980

Table 6. The XRD data

Complex	2θ, deg	d, Å	Relative intensity, %	Particles size, nm
Amox	18.03	4.92	100	155
Au(III)	8.74	10.11	100	4.30

Table 7. Quantum chemical parameters of amox [77–81]

Parameters	Value
Total energy, a. u	–146.14
Binding energy, a. u	–2.97
Heat formation, a. u	2.59
Electronic energy, a. u	–1038.01
Dipole moment, D	2.282
E_{HOMO}, eV	–9.4142
E_{LUMO}, eV	0.4607
ΔE, eV	9.8749
χ, eV	4.4768
η, eV	4.9375
σ, eV	0.2025
P_i, eV	–4.4768
S, eV	0.1013
ω, eV	2.0296
ΔN_{max}, eV	0.9067

TEM analysis demonstrated the presence of nanometric Au(III) ions inclusions in amox molecules (Fig. 4).

Computational studies. Geometry optimization has been performed using semi-empirical PM3 method implemented in Hyperchem 7.5 program [75, 76] (Fig. 5, Table 7).

High values of E_{HOMO} confirmed that amox had a powerful donation character.

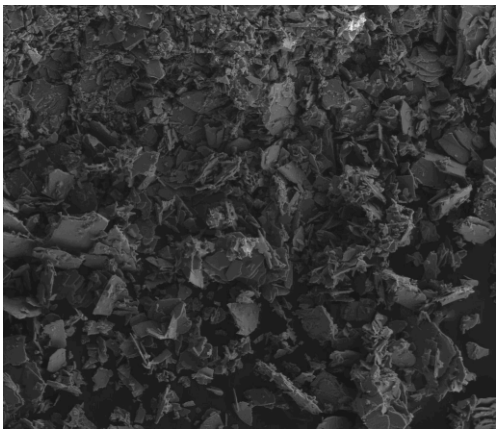

Fig. 3. SEM image of $[Au(amox\text{-}Na)(H_2O)]\cdot Cl_3$ complex.

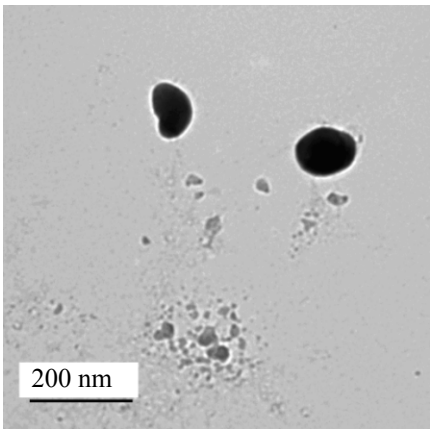

Fig. 4. TEM image of $[Au(amox\text{-}Na)(H_2O)]\cdot Cl_3$ complex.

Table 8. Inhibition zone diameters measured for amox and its complexes tested against some kinds of bacteria and fungi

Sample		Inhibition zone diameter, mm/mg					
		Bacillus subtilis (G^+)	*Escherichia coli* (G^-)	*Pseudomonas aeruginosa* (G^-)	*Staphylococcus aureus* (G^+)	*Aspergillus flavus* (Fungus)	*Candida albican* (Fungus)
Control: DMSO		0.0	0.0	0.0	0.0	0.0	0.0
Standard	Tetracycline Antibacterial agent	34	32	34	30	–	–
Standard	Amphotericin B Antifungal agent	–	–	–	–	18	19
Amox		34	30	33	20	0	0
Ca(II) complex		21	12	28	16	0	0
Fe(III) complex		16	21	21	19	0	0
Pd(II) complex		19	11	17	22	0	0
Au(III) complex		36	18	34	24	2	5

Table 9. The Au(III) complex inhibitory activity against colon carcinoma and hepatocellular carcinoma cells

Concentration, μg	Viability			
	HepG-2 cell line		HCT-116 cell line	
	doxorubicin	Au(III)	doxorubicin	Au(III)
50.000	4.91	10.97	6.82	12.84
25.000	8.87	17.84	8.89	19.53
12.500	14.83	35.73	14.83	38.97
6.250	16.16	64.92	16.16	79.22
3.125	25.28	83.11	22.28	89.13
1.560	34.64	91.59	34.64	95.48
0.780	45.79	96.72	45.78	98.71
0.390	51.08	98.94	51.28	100.00
0.000	100.00	100.00	100.00	100.00
IC_{50}	0.467	9.44	0.471	10.80

Antimicrobial assessments. Antimicrobial tests of free amox and its Ca(II), Fe(III), Pd(II), and Au(III) complexes were carried out against Gram (+) bacteria (*Staphylococcus Aureus, Bacillus subtilis*) Gram (–) bacteria (*Escherichia Coli*, *Pseudomonas aeruginosa*) and Fungi (*Candida Albicans* and *Aspergillus flavus*) with the standards tetracycline as antibacterial agent and amphotericin B as antifungal agent (Table 8). The Au(III) complex demonstrated biological activity higher than the standards probably due to higher lipophilic character of Au(III) ion than that of free ligand and other complexes. Such effect could be interpreted in terms of overtone's concept of cell permeability and Tweedy's chelation theory [82]. *In vitro* cytotoxicity assessment of the Au(III) complex was performed on human colon carcinoma (HCT-116) cell line and human hepatocellular carcinoma (HepG-2) cell line in the presence of doxorubicin standard

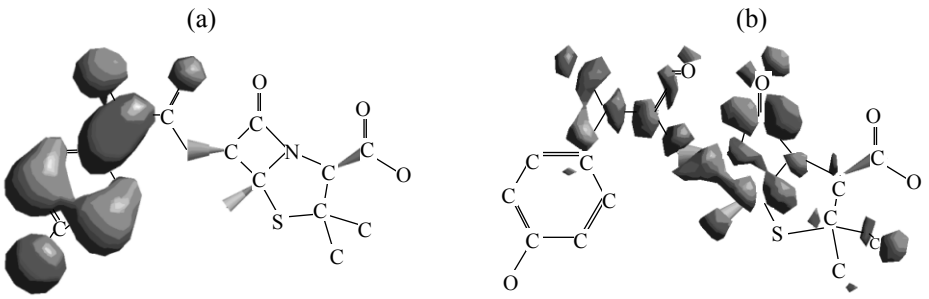

Fig. 5. (a) HOMO and (b) LUMO of amox.

drug. The evaluated data for IC_{50} (Table 9) demonstrated that the Au(III) complex was more effective aganist HepG-2 cell line than HCT-116 cell line.

ACKNOWLEDGMENTS

This work was funded by Deanship of Scientific Research at university of Princess Nora Bint Abdul Rahman.

REFERENCES

1. Abd El–Wahed, M.G., El–Megharbel, S.M., El–Sayed, M.Y., Zahran, Y.M., and Refat, M.S., *Russ. J. Gen. Chem*., 2013, vol. 83, pp. 2438–2446.
2. Refat, M.S., Mohamed, G.G., Ibrahim, M.Y.S., Killa, H.M.A., and Fetooh, H., *Russ. J. Gen. Chem*., 2013, vol. 83, pp. 2479–2487.
3. Zaky, M., El–Sayed, M.Y., El–Megharbel, S.M., Taleb, S.A., and Refat, M.S., *Russ. J. Gen. Chem*., 2013, vol. 83, pp. 2488–2501.
4. Al–Saif, F.A., and Refat, M.S., *Russ. J. Gen. Chem*., 2014, vol. 84, pp. 143–156.
5. Refat, M.S., and Kobeasy, M.I., *Russ. J. Gen. Chem*., 2014, vol. 84, pp. 767–774.
6. Salaman, M., Refat, M.S., El–Korashy, S.A., and Hussien, M.A., *Russ. J. Gen. Chem*., 2014, vol. 84, pp. 1841–1846.
7. Ming, L., *Med. Res. Rev*., 2003, vol. 23, pp. 697–762.
8. Turel, I., *Coord. Chem Rev*., 2002, vol. 232, pp. 27–47.
9. Drevenski, P., Golobic, A., Turel, I., Poklar, N., and Sepcic, K., *Acta Chim. Slov*., 2002, vol. 49, pp. 857–870.
10. King, D.E., Malone, R., and Lilley, S.H., *Am. Fam. Physicians*, 2000, vol. 61, pp. 2741–2748.
11. Srivastava, R.S., *Inorg. Chim. Acta*, 1981, vol. 55, pp. L71–L74.
12. Kopf–Maier, P., *Eur. J. Clin. Pharmacol*., 1994, vol. 47, pp. 1–16.
13. Michael, I.P., *The Chemistry of β-Lactams*, Glasgow, Chapman &Hall, 1992.
14. Zayed, M.A. and Abdallah, S.M., *Spectrochim Acta A*, 2005, vol. 61, pp. 2231–2238.
15. Boles, M.O., Girven, R.J., and Gane, P.A.C., *Acta Crystallogr. B*, 1976, vol. 34, pp. 461–466.
16. Castanheira, M., Sader, H., Desphande, S., Lalitagauri, M., Thomas, R., and Jones, R.N., *Antimicrob. Agents Chemotherap*., 2008, vol. 52, pp. 570–573.
17. Subramanian, S., Roberts, C.L., Anthony, C.H., Martin, M.H., Edwards, W.S., Rhodes, M.J., and Campbell, B., *Antimicrob. Agents Chemotherap.*, 2009, vol. 52, pp. 427–434.
18. Neal, M.J., *Medical Pharmacology at a Glance*, Oxford: Blackwell, 1991, 2 ed. p. 78.
19. Neuman, M. and Degli, V., *Antibioticied Agenti Chemioterapici Anti–Infettivi*, Rome: Sigma-Tau, 1994, p. 133, 5 ed.
20. Campoli–Richards, D.M., and Brogden, R.N., *Drugs*, 1987, vol. 33, pp. 577–609.
21. Cort, W.M., Scott, J.W., Araujo, M., Mergens, W.J., Cannalonga, M.A., Osadca, M., Harley, H., Parrish, D.R., and Pool, W.R., *J. Am. Oil Chemists Soc*., 1975, vol. 52, pp. 174–178.
22. Seunjae, L., Yoshiki, M., Masashi, M., Hiroshi, O., and Kuniyo, I., *J. Biochem.*, 2006, vol. 139, pp. 1007–1015.
23. Bhatia, M.S., Kashedikar, S.G., and Chaturvedi, S.C., *Ind. Drugs*, 1996, vol. 33, pp. 213–218.
24. Satoskazr, R.S. and Bhandarkar, S.D., *Pharmacology and Pharmacother Apeutics,* Bombay: Popular Prakashan, 1990, vol. 2, 11 ed., p. 549.
25. Rang, H.P., *Pharmacology*, London: Churchil Livinston Pub., 1996, 3 ed., p. 691.
26. Dalc, M.M., *Pharmacology*, London: Churchil Livinston Pub., 1998, 3 ed., p. 725.
27. Fleming, P.C., Goldner, M., and Glass, D.G., *J. Bacteriol*., 1969, vol. 98, pp. 394–397.
28. Baczkowicz, M., Wojtowicz, D., Anderegg, J.W., Schilling, C.H., and Tomasik, P., *Carbohydr. Polym*., 2003, vol. 52, pp. 263–268.

29. Delgado, J. and Remers, W.A., *Textbook of Organic Medicinal and Pharmaceutical Chemistry*, J. Lippincott Co., 1991, 9 ed., p. 244.
30. Lyle, S.L. and Yassin, S.S., *Analytica. Chim. Acta*, 1993, vol. 274, pp. 225–230.
31. Pellerito, L., Maggio, F., Consiglio, M., Pellerito, A., Stocco, G.C., and Grimaudo, S., *App. Organomet. Chem*., 1995, vol. 9, pp. 227–239.
32. Stefano, R.D., Scopelliti, M., Pellerito, C., Fiore, T., Vitturi, R., Colomba, M.S., Gianguzza, P., Stocco, G.C., Consiglio, M., and Pellerito, L., *J. Inorg. Biochem*., 2002, vol. 89, pp. 279–292.
33. Imran, M., Iqbal, J., Mehmood, T., and Latif, S., *J. Biological Sciences*, 2006, vol. 6, pp. 946–949.
34. Khallowa, K.I. and Al–Omari, N.A., *Tikrit J. Pure Sci*., 2008, vol. 13, pp. 152–155.
35. Kumar, K. and Mishra, P., *Main Group Chemistry*, 2008, vol. 7, pp. 1–14.
36. Mishra, P., *Int. J. ChemTech Res*., 2009, vol. 1, pp. 401–419.
37. Joshi, S., Pawar, V., and Uma, V., *Int. J. Pharma. Bio. Sci*., 2011, vol. 2, pp. 240–250.
38. Alekseev, V.G. and Zamyslov, V.G., *Russ. J. Coord. Chem*., 2007, vol. 33, pp. 254–257.
39. Arefi, D., Maknoni, F., and Khoshnood, R.S., *Clin. Biochem.*, 2011, vol. 44, pp. S265.
40. Refat, M.S., Kobeasy, M.I., and El-Shazly, M.A., *Russ. J. Gen. Chem*., 2014, vol. 84, pp. 1411–1416.
41. Zaky, M., El-Sayed, M.Y., El-Megharbel, S.M., Taleb, S.A., and Refat, M.S., *Russ. J. Gen. Chem*., 2015, vol. 85, pp. 176–184.
42. Al-Khodir, F.A.I. and Refat, M.S., *Russ. J. Gen. Chem*., 2015, vol. 85, pp. 718–730.
43. Al-Khodir, F.A.I. and Refat, M.S., *Russ. J. Gen. Chem*., 2015, vol. 85, pp. 1734–1744.
44. El-Megharbel, S.M., Adam, A.M.A., Megahed, A.S., and Refat, M.S., *Russ. J. Gen. Chem*., 2015, vol. 85, pp. 2366–2373.
45. El–Megharbel, S.M., Hamza, R.Z., and Refat, M.S., *Chem.-Biol. Interact.*, 2014, vol. 220, pp. 169–180.
46. Bauer, A.W., Kirby, W.M., Sherris, C., and Turck, M., *Am. J. Clinical Pathology*, 1966, vol. 45, pp. 493–496.
47. Pfaller, M.A., Burmeister, L., Bartlett, M.A., and Rinaldi, M.G., *J. Clin. Microbiol*., 1988, vol. 26, pp. 1437–1551.
48. *National Committee for Clinical Laboratory Standards*, Performance vol. antimicrobial susceptibility of Flavobacteria, 1997.
49. *National Committee for Clinical Laboratory Standards*, Methods for dilution antimicrobial susceptibility tests for bacteria that grow aerobically. Approved standard M7–A3. National Committee for Clinical Laboratory Standards, Villanova, Pa, 1993.
50. *National Committee for Clinical Laboratory Standards*, Reference Method for Broth Dilution Antifungal Susceptibility Testing of Conidium–Forming Filamentous Fungi: Proposed Standard M38–A. NCCLS, Wayne, PA, USA., 2002.
51. *National Committee for Clinical Laboratory Standards*, Methods for Antifungal Disk Diffusion Susceptibility Testing of Yeast: Proposed Guideline M44-P. NCCLS, Wayne, PA, USA, 2003.
52. Liebowitz, L.D., Ashbee, H.R., Evans, E.G.V., Chong, Y., Mallatova, N., Zaidi, M., Gibbs, D., and Global Anti-fungal Surveillance Group, *Diagn. Microbiol. Infect. Dis*., 2001, vol. 4, pp. 27–33.
53. Matar, M.J., Ostrosky–Zeichner, L., Paetznick, V.L., Rodriguez, J.R., Chen, E., and Rex, J.H., *Antimicrob. Agents Chemother*., 2003, vol. 47, pp. 1647–1651.
54. Mosmann, T., *J. Immunol. Methods*, 1983, vol. 65, pp. 55–63.
55. Gangadevi, V. and Muthumary, J., *African J. Biotechnology*, 2007, vol. 6, pp. 1382–1386.
56. Refat, M.S., *Spectrochimica Acta, A*, 2007, vol. 68, pp. 1393–1405.
57. Nakamoto, K., *Infrared and Raman Spectra of Inorganic and Coordination Compound*, New York: Wiley, 1978.
58. Kanooco, N., Singh, R.V., and Tandon, J.P., *Syn. React. Inorg. Met. Org. Chem*., 1987, vol. 17, pp. 837–847.
59. Deacon, G.B. and Phillips, R. J., *Coord. Chem. Rev*., 1980, vol. 33, pp. 227–250.
60. Anacona, J.R. and Figueron, E.M., *J. Coord. Chem*., 1999, vol. 48, pp. 181–189.
61. Ozturk, O.F., Sekerci, M., and Ozdemir, E., *Russ. J. Coord. Chem*., 2005, vol. 31, pp. 651–654.
62. Ozturk, O.F., Sekerci, M., and Ozdemir, E., *Russ. J. Gen. Chem*., 2006, vol. 76, pp. 33–36.
63. Ghiladi, R.A., Kretzer, R.M., Guzei, I., Rheingold, A.L., Neuhold, Y., Hatwell, K.R., Zuberbuhler, A.D., and Karlin, K.D., *Inorg. Chem*., 2001, vol. 40, pp. 5754–5767.
64. Hamada, Y.Z., Carlson, B.L., and Shank, J.T., *Synth. & React. Inorg. Met–Org. Chem*., 2003, vol. 33, pp. 1425–1440.
65. Cotton, F.A., Goodgame, D.M.L., and Goodgame, M., *J. Am. Chem. Soc*., 1962, vol. 84, pp.167–172.
66. Figgis, B.N., *Introduction to Ligand Fields*, New York: John Wiley and Sons, 1967, pp.285.
67. Abdalrazaq, E.A., Buttrus, N.H., and Abd Al-Rahman, A.A., *Asian J. Chem*., 2010, vol. 22, pp. 2179–2186.
68. Ibrahim, E.S., Sallam, S.A., Orabi, A.S., El-Shetary, B.A., and Lentz, A., *Monatshefte fur Chemie*, 1998, vol. 129, pp. 159–171.

69. Coats, A.W. and Redfern, J. P., *Nature*, 1964, vol. 201, pp. 68–69.
70. Yusuff, K.K.M. and Sreekala, R., *Thermochim Acta*, 1990, vol. 159, pp. 357–368.
71. Frost, A.A. and Peasron, R.G., *Kinetics and Mechanism*, New York: Wiley, 1961.
72. Cullity, B.D., *Elements of X-Ray Diffraction*, Addison-Wesley, Reading, MA, 1972, p. 102.
73. Salavati–Niasari, M., Mohandes, F., Davar, F., Mazaheri, M., Monemzadeh, M., and Yavarinia, N., *Inorg. Chim. Acta*, 2009, vol. 362, pp. 3691–3697.
74. Velumani, S., Mathew, X., and Sebastian, P.J., *Solar Energy Mater. Solar Cells*, 2003, vol. 76, pp. 359–368.
75. Helal, M.H., El–Awdan, S.A., Salem, M.A., Abd-elaziz, T.A., Moahamed, Y.A., El–Sherif, A.A., and Mohamed, G.A.M., *Spectrochim. Acta Part A*, 2015, vol. 135, pp. 764–773.
76. Hyper Chem. Version 7.51 Hyper cube, INC.
77. Pearson, R.G., *J. Org. Chem*., 1989, vol. 54, pp. 1423–1430.
78. Geerlings, P., De Proft, F., and Langenaeker, W., *Chem. Rev*., 2003, vol. 103, pp. 1793–1873.
79. Parr, R.G., *J. Am. Chem. Soc*., 1999, vol. 121, pp. 1922–1924.
80. Chattaraj, P.K. and Giri, S., *J. Phys. Chem. A*, 2007, vol. 111, pp. 11116–11121
81. Speie, G., Csihony, J., Whalen, A.M., and Pie-Pont, C.G., *Inorg. Chem*., 1996, vol. 35, pp. 3519–3535.
82. Raman, N., Kulandaisamy, A., and Thangaraja, C., *Trans. Metal Chem*., 2004, vol. 29, pp. 129– 135.